Trolls: a novel low-cost controlling system platform for walk-behind tractor

Padma Nyoman Crisnapati[1,2], Dechrit Maneetham[1], Evi Triandini[2]

[1]Department of Mechatronics Engineering, Faculty of Technical Education, Rajamangala University of Technology Thanyaburi, Pathum Thani, Thailand

[2]Department of Information System, Faculty of Informatics and Computers, Institute of Technology and Business STIKOM Bali, Bali, Indonesia

Article Info

ABSTRACT

A novel low-cost controlling system platform for walk-behind hand tractors (Quick G3000 and G1000) was designed and developed to solve the fatigue problem faced by farmers when ploughing the rice field. This platform is dedicated to designing and manufacturing mechanical, electrical, and software components. The tractor was modified and added with an embedded control system that functioned as the slave, while the direction of the tractor movement was controlled remotely by humans through Bluetooth communication with the smartphone application as the master. Several servos and direct currents (DCs) were used as the actuator to move some levers and clutches instead of the tractor to make it remotely controllable. This system has been directly tested in the paddy farming land through two tractors: Quick G3000 and G1000. The testing results showed that this system could be used within more or less six hours; there is a cost-efficiency of 21.74% and 84.62% battery usage efficiency. More efficient mechanics caused this cost efficiency, and the reduction in electronic devices affects battery efficiency. A low-cost platform for controlling walk-behind tractors has been successfully developed; this platform assists farmers in ploughing their fields.

This is an open access article under the CC BY-SA license.

Corresponding Author:

Dechrit Maneetham
Department of Mechatronics Engineering, Faculty of Technical Education, Rajamangala University of Technology Thanyaburi
39 Village No. 1 Rangsit - Nakhon Nayok Road, Tambon Khlong Hok, Amphoe Thanyaburi Pathum Thani 12110, Thailand
Email: dechrit_m@rmutt.ac.th

1. INTRODUCTION

In several provinces in Indonesia, two-wheel walk-behind hand tractors have been widely used by farmers. This tractor has a "V" shape, and on the tip of the control, there is a handle used to turn the tractor left or right; it uses gasoline. However, the controlling process is still done manually by human operators interacting with the tractor [1]. When seen from the area of agricultural land to be ploughed, this process certainly can make the farmer operators tired of controlling the tractor for a long time, particularly in scorching weather. These problems even can make farmers feel tired quickly during the tillage process and make tractor operation inefficient.

Several studies in control systems have been conducted on the two and four-wheeled tractors to cope with these problems. A multi-modal dataset was compiled utilizing a variety of cameras and sensors to detect static and moving objects to serve as the foundation for the development of automated agricultural

vehicles [2]. Research on precise point positioning (PPP) in precision agriculture (PA) was also conducted utilizing global navigation satellite system (GNSS) technology on big four-wheel tractors [3]–[6]. Several of these studies have resulted in the development of a four-wheel tractor control system at a relatively high cost to Indonesian farmers [7]–[10]. Furthermore, numerous studies have been conducted to optimize the tractor's mechanical performance [11]–[17], embedded control systems [18]–[23], and software [24]–[28], enabling it to operate and be controlled by a distance. These comprehensive studies are focused on powerful four-wheeled tractors.

This study presents a novel design, implementation, and testing on the low-cost trolls (tractor controlling system) platform for a small two-wheel-drive walk-behind hand tractor (Quick G3000 and G1000). Based on our knowledge, this is the first time a remote-control system has been used to operate this type of tractor from a certain distance. The control command was sent via Bluetooth, and the HC-05 module was utilized as the receiver in Arduino. This platform was tested in the Quick G3000 and G1000 tractors. These tractors were selected considering that many farmers in Indonesia use this tractor. This research has two main contributions; the first is the novel design and implementation of the mechanics, electronics, and software of the G3000 and G1000 tractors. The system prototype was implemented in G3000, and the commercialized ready final product was implemented in G1000.

With this platform, farmers can control their tractors remotely using smartphones to plough rice fields without having to heat up and experience fatigue. The maximum control distance is 30 meters due to the Bluetooth's signal range limitation. The second contribution is the tractor's mathematical model, used to simulate the tractor movement using two controllers comparison, namely pure pursuit control (PPC) and supervisory logic control (SLC). This model creates tractor behaviour and movement simulations in the MATLAB application. A pure pursuit controller algorithm moves the tractor model simulation autonomously from one coordinate to another. A pure pursuit controller was chosen because using a high-speed tractor in the rice field tillage process is unnecessary; this algorithm is solid and easy to implement [29], [30]. We also use a supervisory logic controller to compare [31], [32]. The simulation results are made using MATLAB/Simulink, and some experiments are presented and discussed. As a preliminary study, we collect data from global positioning system (GPS) and compass sensors with the internet of things technology in the field-testing process. Because the data obtained has a lot of noise and is less stable, filtering is needed. We compared two filters (Kalman and Butterworth low pass) to find the best possible one.

2. RESEARCH METHOD
2.1. Mechanical design and development
Several modifications were made to the quick walk-behind hand tractor manufacturer with the G3000 and G1000 types. Changes were made to five parts of the tractor, i.e., head of handle bar, steering linkage, tension handle, throttle lever, and main pipe. Figure 1(a) illustrates the position of the four parts, while the fifth part, the throttle lever, as shown in Figure 1(b).
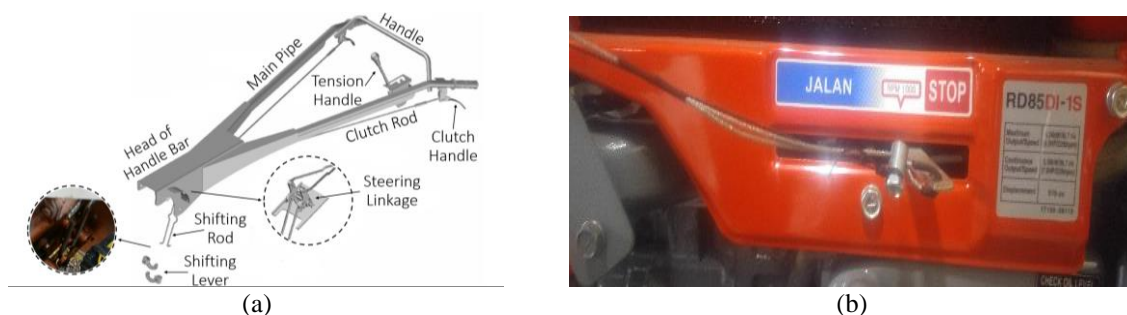

(a)   (b)

Figure 1. Position of (a) parts of handle bar and (b) throttle lever of the Quick G3000 tractor

2.1.1. Walk-behind hand tractor
The two-wheel walk-behind hand tractor is a farm machine that can be used for tillage and other agricultural work with a draft device installed on the back of the machine. Compared to bull power, this machine has high efficiency [33]. It is a multipurpose machine since it can also function as a driver for water pumps, processing equipment, or trailers. The tractor must be equipped with tillage equipment, such as a chop, harrow, or rotary plough as a ploughing machine. In Indonesia, hand tractors with V-shaped frames

such as Quick G3000 and G1000 are the most widely used machines in the process of ploughing rice fields [34]–[36].

2.1.2. Tractor movement

The G3000 and G1000 tractors have a similar movement control mechanism. Both use two wheels to maneuver over paddy fields. Each wheel is driven by pulling two clutch handles independently or simultaneously. The steering linkage, shifting rod, and shift lever are moved when the clutch handle is retracted. The tractor turns left when the left clutch handle is pulled and vice versa when the right clutch handle is pulled. If the operator does not pull both, the tractor continues straight; nevertheless, the tractor comes to a complete stop if both are pulled. The tractor's direction of movement is depicted in Figure 2.
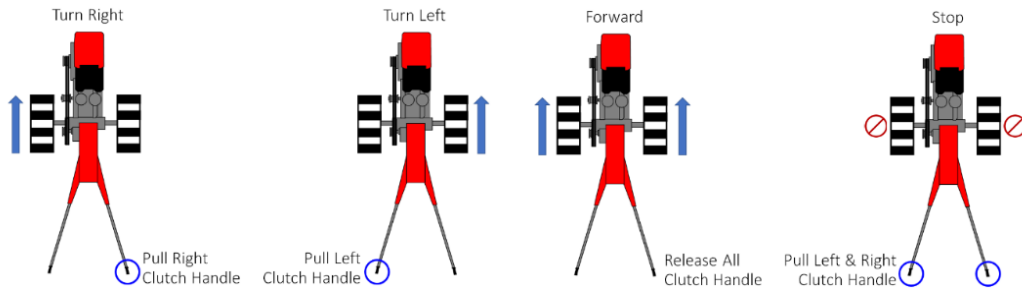
Figure 2. The direction of the tractor movement is based on the pulled clutch handle

2.1.3. Handle bar head and steering linkage

In the handlebar head tractor G3000, four servo motors and two pulleys were added. This device is divided into two parts and arranged on the right and left parallel. As shown in Figure 3, each piece consists of two servo motors and one pulley. The servo motor and pulley are connected to the steering linkage using a stainless-steel wire rope, as in Figure 4. With this design, the tractor can be controlled to the right and left using the movement of the servo motors.

After analyzing the field testing of the prototype design, the costs incurred for the purchase of four servos were found to be relatively high for the farmers. Hence, an improvement was made to the mechanical design of the G1000 tractor by using only one servo motor on each right or left side and removing the use of pulleys. As shown in Figure 5, the servo motor is directly connected to the clutch handle end.
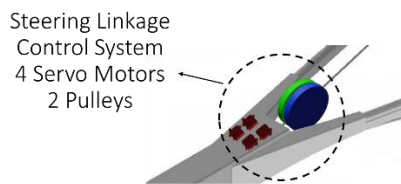
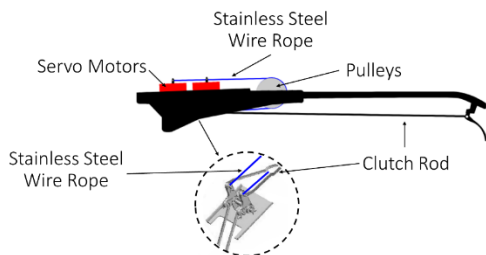Figure 3. Head of handle bar modification design

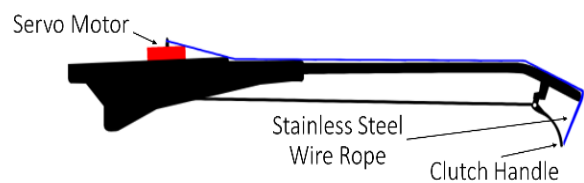Figure 4. G3000 wire connection between servo motors, pulleys, and steering linkage design

Figure 5. G1000 wire connection between servo motor and cultch handle design

2.1.4. Tension handle

The tension handle is used to manage the tightness of the V-Belt on the tractor. The tighter the V-Belt, the more speed, and thrust increase. This part can be moved by pulling back or pushing forward, as shown in Figure 6. Therefore, a modification made to the G3000 and G1000 tractors was by adding a direct current (DC) motor with the concept of a screw system for linear movement.

2.1.5. Throttle lever

Aside from managing the tension handle, farmers can adjust the tractor's speed and thrust by shifting the throttle lever to the right and left. To be controlled remotely, the modification was made by adding a DC motor. The screw system for the linear movement was used to make the rotation of the motor will be converted into a right and left shifting motion. Figure 7 shows the throttle lever feeding modifications on the G3000 tractor. The prototype design required a long time to move the throttle lever based on the field testing results. Based on this problem, a change was given and implemented to the G1000 tractor. The DC motor was installed without using a screw system for the linear movement concept in this design. Figure 8 presents the results of the revision design implementation.
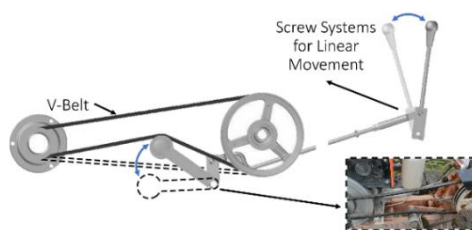
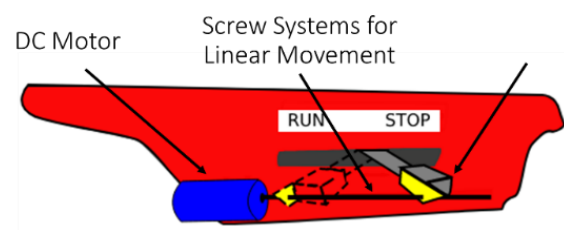Figure 6. Tension handles mechanical structure for G1000 and G3000

Figure 7. Throttle lever mechanical modification design for G3000 tractor

2.1.6. Main bar

By default, the G 3000 and G 1000 tractors have a retainer in the front to prevent them from falling forward; the front of the tractor is heavier in the absence of a counterweight in the rear. Modifications to the main bar are made by utilizing rubber wheels that are not used when the tractor is in ploughing mode and are equipped with iron wheels shown in Figure 9. With this modification, the tractor maintains a good balance and does not become stuck or sink into the mud when applied forward or reverse momentum. The tractor weight balancing hanger is installed on the main pipe near the clutch handle to ensure that the tractor balances independently of the operator. This hanger has a maximum capacity of two rubber wheels.
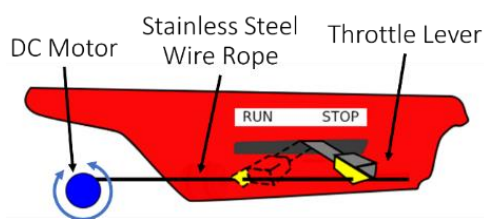
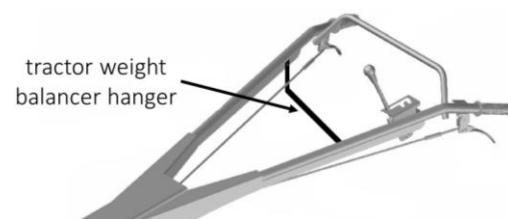Figure 8. Throttle lever mechanical modification design for G1000 tractor

Figure 9. Tractor weight balancer hanger design

2.2. Electrical driver unit design

The electrical driver unit is a part that acts to manage the movement of the tractor based on the input received from the mobile application. This unit consists of an Arduino Uno microcontroller as the primary control device for several actuators. Several servo motors with a torque of 25 kg-cm were used to control the tractor movement to the left or right. For the G3000 tractor, four servos were used, while the G1000 tractor only used two servos. DC motor was used to control the tension handle and throttle lever with a voltage of 12 V and a torque of 10 kg-cm. A motor driver with type H-Bridge BTS7960 was used for these two DC motors. The HC-05 Bluetooth module communicated between the driver unit and the mobile application.

The power source to use is a 12 V battery with a capacity of 7 Ah. Some electronic modules require lower voltages, and in this design, two step-downs were used to lower the voltage from 12 to 5 and 6 V. Figure 10(a) illustrates the wiring diagram of the driver unit. After completing the field test, we simplified the electronic component circuit into a single microcontroller board. As preliminary research, a GPS sensor (Ublox 6M) and a Compass (HMC5883L) were installed to obtain tractor location and orientation data using TTGO-TCall ESP32 SIM800L internet of things (IoT) technology, details of the circuit can be seen in Figure 10(b). We compared the two filters to reduce sensor reading noise, namely the Kalman Filter and the Butterworth low pass filter (LPF).
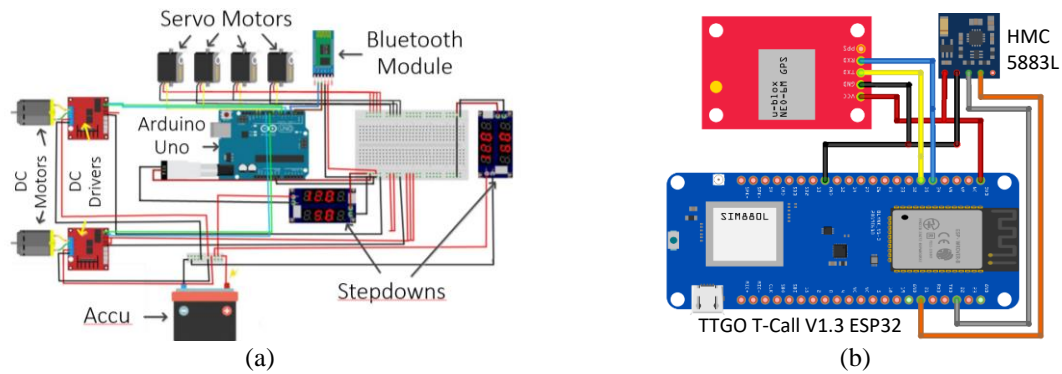

Figure 10. Wiring diagram for (a) driver unit and (b) GPS+ compass logger

2.3. Software development
2.3.1. Arduino software

Software embedded in the Arduino functioned as the slave to receive the message sent by the Android software through Bluetooth communication. The message received was then identified to obtain a set of sequence commands to do the updated value towards several actuators such as DC or servo motors. After the message was identified, the command was issued to write the message's value to each actuator and drive the tractor. Figure 11 depicts the flow diagram between Arduino and Android.

2.3.2. Android software

Android software acts as the master message sender to Arduino. This software shows the list of Bluetooth available surroundings and then connects them. Once connected, the users can select the available commands, as shown in Figure 12. The set commands are then sent in a message through Bluetooth communication.
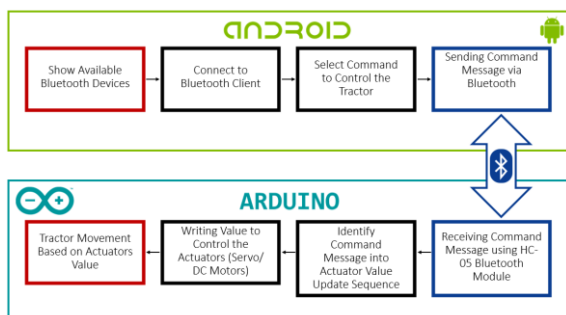

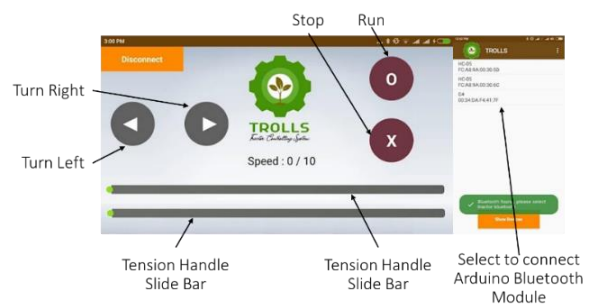Figure 11. Flow diagram of Arduino and android software

Figure 12. Final android application user interface for tractor remote controlling system

2.3.3. Filter comparison for GPS and compass data

As preliminary research on an autonomous tractor, sensor readings and filter comparison are needed to record the tractor's behavior. GPS and compass are usually used for a vehicle to perform trajectory

tracking. From these two sensors, several data are obtained regarding the position and orientation of the tractor. Still, the data obtained by the Ublox 6M and HMC5883L have noise and are very unstable. A filtering technique is applied to overcome this problem. Kalman filter and Butterworth LPF are used to seeing the optimal filter results to reduce the noise of the two sensors.

In using the Kalman Filter, the process (system) can be modelled in (1) with the measurement (sensor) model in (2). The noises in the predictions and measurement procedures were determined by measuring the shift and comparing it to predicted and measured data using the minimal error approach. See (3) for the covariance matrix of w_k and v_k (Q and R, respectively) derived from the inaccuracy in predicted and measured changes compared to manually measured changes [37]. Using the linear Kalman model, P_k (6) [37] represents the error covariance between x_k, $\hat{x}_k$ (4), and (5) [37]. As shown in (7) gives the value of the Kalman gain (K_k) that minimizes the sum squared error [37], H_k and k is constant. Algorithm 1 is the application of the Kalman filter.

$$x_{k+1} = \varphi_k x_k + w_k \tag{1}$$

$$U = y_k = H_k x_k + v_k \tag{2}$$

$$Cov(wk) = Q_{kalman}, Cov(vk) = R_{kalman} \tag{3}$$

$$x_k = \hat{x}_k = \hat{U} \tag{4}$$

$$\hat{U} = \hat{U} + K_k[U - H \cdot \hat{U}] \tag{5}$$

$$P_k = (1 - K_k \cdot H_k)P_k + Q_{kalman} \tag{6}$$

$$K_k = P_k \cdot H_k (H_k \cdot P_k \cdot H_k + R_{kalman})^{-1} \tag{7}$$

Where, x_k the state vector, φ_k the state transition matrix, which connects the next time step's state vector to the current state, w_k process noise, v_k the measurement noise, P_k the error covariance between x_k, $\hat{x}_k$, H_k the matrix that connects the measurement vector and the state vector, x_{k+1} the process (system) model, $\hat{U}=\hat{x}_k$ the post estimation of x_k using the linear process model, $U_= y_k$ The measurement (sensor) model, Q_{kalman} the covariance matrix of w_k, R_{kalman} the covariance matrix of v_k, and K_k Kalman gain.

Algorithm 1. Kalman filter

```
Data: φ=1.00, H=1.00, R_kalman=Cov(v_k)=0.33, Q_kalman=Cov(w_k)=15, P_0=0, K_0=0
Result: Û
1.  while true do
2.         ➔ Obtain noisy U₁(at each time step)
3.         ➔ GOTO KALMAN, obtain filtered U₁ (at each time step)
4.  end while
5.  function KALMAN(U)
6.         ➔K_k = (P_k·H_k)/(H_k·P_k·H_k+R_kalman)  (update Kalman Gain)
7.         ➔Û = Û + K_k[U − H · Û]
8.         ➔P_k = (1− K_k · H_k) P_k+Q_kalman
9.         ➔
10. return Û;
```

The Butterworth low pass filter provides maximum passband evenness, to be called an anti-aliasing filter. The higher the filter order, the longer the bandpass evenness. The general form of the transfer function model of a second-order Butterworth low pass filter can be described by n (8) [38]. The polar form of the low pass filter is given by (9) [38]. The application of this filter can be seen in Algorithm 2.

$$H(s) = \frac{K}{s^2 + 2\zeta\Omega_c s + \Omega_c^2} \tag{8}$$

$$\left|\frac{Output}{Input}\right| = \frac{K}{\sqrt{1+\left(\frac{f}{f_h}\right)^4}} \tag{9}$$

Where, $H(s)$ Butterworth transfer function, Ω_c natural frequency, K gain in passband, f_h cutoff frequency, ζ the damping ratio of the system, s the plane, and f input frequency.

Algorithm 2. Butterworth low pass filter

```
Data: nzeros= 2, npoles= 2, gain=8.524410156e+00, xv[nzeros+1], yv[npoles+1],
      next_input_value, next_output_value
Result: next_input_value
1.  while true do
2.          ➔ Obtain noisy next_input_value (at each time step)
3.          ➔ GOTO ButterworthLPF, obtain filtered next_input_value (at each time step)
4.  end while
5.  function ButterworthLPF(next_input_value)
6.          ➔xv[0] = xv[1]; xv[1] = xv[2];
7.          ➔xv[2] = next_input_value / gain;
8.          ➔yv[0] = yv[1]; yv[1] = yv[2];
9.          ➔yv[2] = (xv[0]+xv[2])+2*xv[1]+(-0.2947082939*yv[0])+(0.8254676161*yv[1]);
10. return(next_output_value = yv[2]);
```

2.3.4. Simulation design of walk-behind tractor

This research carried out the kinematic mathematical modelling of the walk-behind hand tractor with the two-wheel differential drive. This kinematic model is used for simulation using the pure pursuit and supervisory logic control algorithm with the waypoint concept in the MATLAB/Simulink application. The kinematic model is based on the tractor types of G 3000 and G 1000. Both have two independently driven wheels that can control velocity and angularity and are also known as differential drive vehicles. A mathematical model of the tractor itself is needed to study and simulate the behavior (operation of the walk-behind hand tractor); it is essential to do this before field testing is carried out. When modelling a tractor, the following two assumptions are made. The first assumption is that the tractor is moving at a constant speed. Second, the tractor wheels do not slip, and the surface for robot movement is flat. Figure 13 is a general description of the tractor model, which is used as the basis for the kinematics model of (10)-(13) with a differential drive type [39]. A walk-behind hand tractor kinematics model can be written from this equation, a function of the left and right wheel angular velocity in a matrix (14). As shown in (15) and (16) are forward kinematics calculations to relate the forward speed and angle of the tractor to the differential drive [39]. At the same time, (17) and (18) are inverse kinematics to get the value of the angular velocity of the right and left wheels [39]. Both forward kinematics and inverse kinematics equations convert between body speed and wheel speed in visualizing tractor movement in Simulink.

$$\xi = \begin{bmatrix} \dot{x} \\ \dot{y} \\ \dot{\theta} \end{bmatrix} \tag{10}$$

$$\dot{x} = v \cos \theta \tag{11}$$

$$\dot{y} = v \sin \theta \tag{12}$$

$$\dot{\theta} = \omega \tag{13}$$

$$\begin{bmatrix} \dot{x} \\ \dot{y} \\ \dot{\theta} \end{bmatrix} = \frac{1}{2} \begin{bmatrix} R \cdot \cos \theta & R \cdot \cos \theta \\ R \cdot \sin \theta & R \cdot \sin \theta \\ \frac{R}{L} & -\frac{R}{L} \end{bmatrix} \begin{bmatrix} \omega_R \\ \omega_L \end{bmatrix} \tag{14}$$

$$v = \frac{R}{2}(\omega_R + \omega_L) \tag{15}$$

$$\omega = \frac{R}{L}(\omega_R - \omega_L) \tag{16}$$

$$\omega_L = \frac{1}{R}\left(v - \frac{\omega L}{2}\right) \tag{17}$$

$$\omega_R = \frac{1}{R}\left(v + \frac{\omega L}{2}\right) \tag{18}$$

Where, ξ the robot's pose in the local frame, $\dot{x}$ x position, $\dot{y}$ y position, $\dot{\theta}$ the angle of tractor orientation, R the radius of the wheel, ω_R right wheel angular velocity (rad/s), ω_L left wheel angular velocity (rad/s), v linear velocity (m/s), ω angular velocity (rad/s), L distance between the left and right wheels.
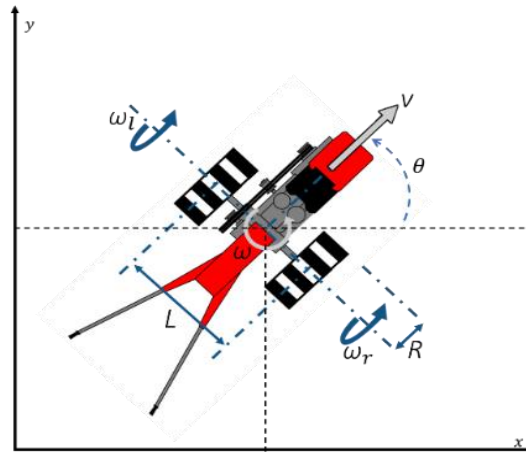
Figure 13. Differential drive kinematic model

3.   RESULTS AND DISCUSSION

This study proposes a novel controlling platform system (mechanical, electrical, and software) for walk-behind hand tractors with a low budget. The operator controls it via an android application using the Bluetooth connection. The prototype design was built and implemented on the G3000 tractor, and it was tested on the farmland. Several revisions were made to obtain the final product's design from the field trial, later implemented and tested on the G1000 tractor. Modifications were made to the standard tractor by adding a novel mechanical and electrical driver unit design to be controlled remotely. In the first experiment (prototype design on the tractor G1000), we used four servo motors and two pulleys connected to the steering linkage using a stainless-steel wire rope, see Figure 14. However, an evaluation of this design resulted in a reasonably high cost and inefficient use of power, so, in the second experiment (the final product design on the G3000 tractor), only two servo motors were used, which were directly connected to the end of the clutch handle, see Figure 15. Novel mechanical design modifications were also applied to the tension handle, see Figure 16 and throttle lever using a screw system for linear movement. This movement system functions optimally on the tension handle in the first and second trials. However, the throttle lever mechanical design was not optimal in the first experiment, see Figure 17, so it was replaced with a DC motor with an encoder, see Figure 18. Another novel mechanical design is applied to the main bar by providing a tractor weight balance hanger, shown in Figure 19. This weight balance hanger design works optimally in the first and second experiments.

Along with the mechanical design, the electrical driver unit functions as a slave, accepting commands and driving the actuator. The initial experiment included standalone or modular electronic components Figure 20(a). This driver unit design requires less cost-efficient; therefore, a single-board microcontroller board combines the functions of several modules into one Figure 20(b). Android software is made as a master to send commands to the driver unit. The software design was made portrait on the first try, but the operator deemed this design less than optimal Figure 21(a). So, based on these shortcomings, the software design was changed to landscape, as shown in Figure 12. The Bluetooth communication protocol is cost-effective and can span numerous agricultural fields in Indonesia, particularly the Bali region. This application has been accessible on the Google Play Store under TROLLS-tractor controlling system (STIKOM Bali developer). This final product was then tested on the farmland, as shown in Figure 21(b). A cost and battery runtime comparison between the prototype and the final product was performed to validate this platform. As shown in Table 1, the test results measured the cost-efficiency of the walk-behind hand tractor controlling system. A 21.74% cost efficiency is obtained from comparing the total cost spent making the final product and the prototype. This cost efficiency showed that shifting the connection of stainless-steel wire rope from the steering linkage to the clutch handle could reduce the number of stepper motors. Also, combining several components into a single board microcontroller could save the cost spent compared to buying several components separately. During the test, the accumulator battery with a voltage of 12 V and capacity of 7 Ah was used. In the prototype design, two batteries were arranged in parallel to fulfill the Current's need, and the final product also used two batteries. Based on the field testing in the farmland, the endurance of the battery runtime could achieve more or less 12 hours. Battery utilization efficiency is 84.62 percent, as determined by the difference between the consumption of the final product and prototype batteries. Table 2 shows the final result of battery usage.
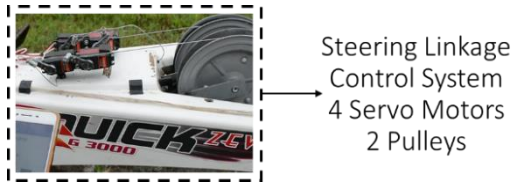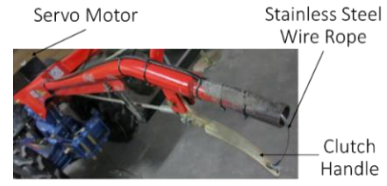
Figure 14. G3000 head handle bar modification

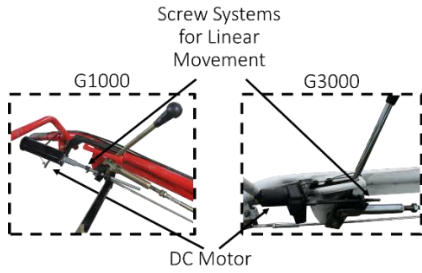Figure 15. G1000 head handle bar modification

Figure 16. Tension handles mechanical modification

Figure 17. G1000 throttle lever mechanical modification

Figure 18. G3000 throttle lever mechanical modification
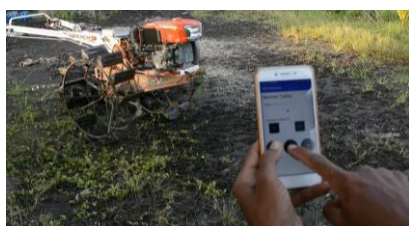

Figure 19. Tractor weight balancer hanger

(a)

(b)

Figure 20. Hardware implementation for (a) control system prototype on G3000 and (b) final product single board microcontroller implemented on G1000

(a)

(b)

Figure 21. Field test of (a) the prototype using a G3000 tractor and (b) the final product using a G1000 tractor

Table 1. The Tractor controlling system production cost (prototype and final product)

Component	Prototype (Qty)	Final Product (Qty)	Price	Prototype ($)	Final Product ($)
Servo motor	4	2	14.5	58	29
DC motor	2	2	20.6	41.2	41.2
Accumulator battery	2	2	15	30	30
Arduino Uno	1	n/a	6	6	n/a
BTS7960 DC driver	2	n/a	4.13	8.26	n/a
Bluetooth HC-05	1	1	3.44	3.44	3.44
Step-down	2	n/a	2.48	4.96	n/a
Single board microcontroller	n/a	1	7.6	n/a	7.6
Approximated turning machine cost	1	1	35	35	35
			Total Cost	186.86	146.24

Table 2. Accumulator battery runtime comparison (prototype and final design)

Component	Prototype (Qty)	Final Product (Qty)	Current Each Component (A)	Prototype (A)	Final Product (A)
Servo Motor	4	2	1.9	7.6	3.8
DC Motor	2	2	1.4	2.8	2.8
			Total Current (A)	10.4	6.6
		Approximated Battery Run Time (Real-time Field Testing) (Hours)		6.5	12

We also track the tractor location and orientation, apart from measuring cost efficiency and battery runtime. Data from GPS and compass sensors (HMC5883L) were collected during the field test. The Kalman and Butterworth low pass filter were then applied with visualizations, as Figures 22 and 23. The two images show that the data generated from GPS and compass is volatile; therefore, the filter can produce stable data. However, from these two images, the comparison results between the Kalman and Butterworth low pass filters cannot be seen, so a root-mean-square error (RMSE) test is carried out on position and orientation predictions with different durations using (19) [40], where $M_n(X_n)$ is the actual measurement based on X_n, $M_n^p(x_n)$ is the prediction time, and N is the number of prediction times. From this test, see Table 3, it can be concluded that the second-order Butterworth low pass filter gets better results when compared to the Kalman filter.

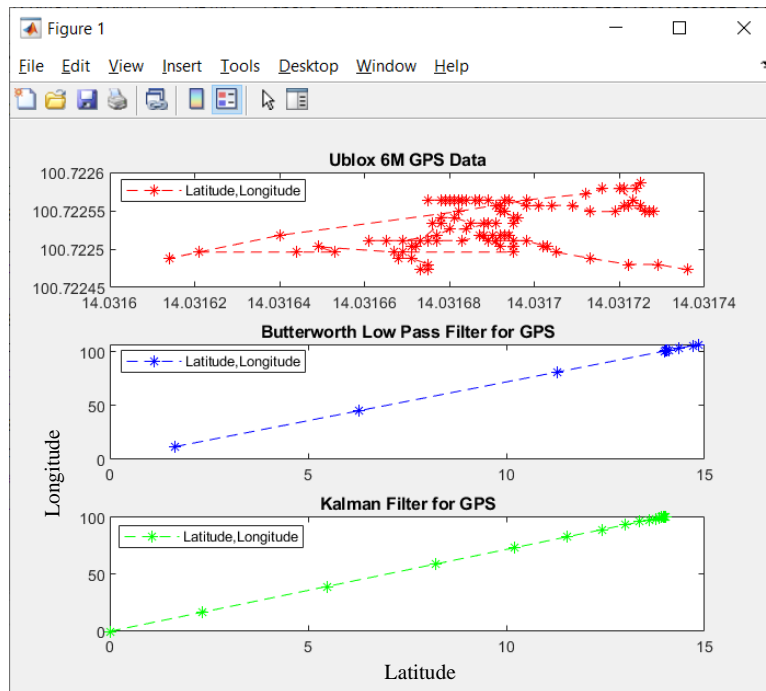$$RMSE = \sqrt{\frac{1}{N}\sum_{n=1}^{N}\left(M_n^p(x_n) - M_n(X_n)\right)^2} \qquad (19)$$
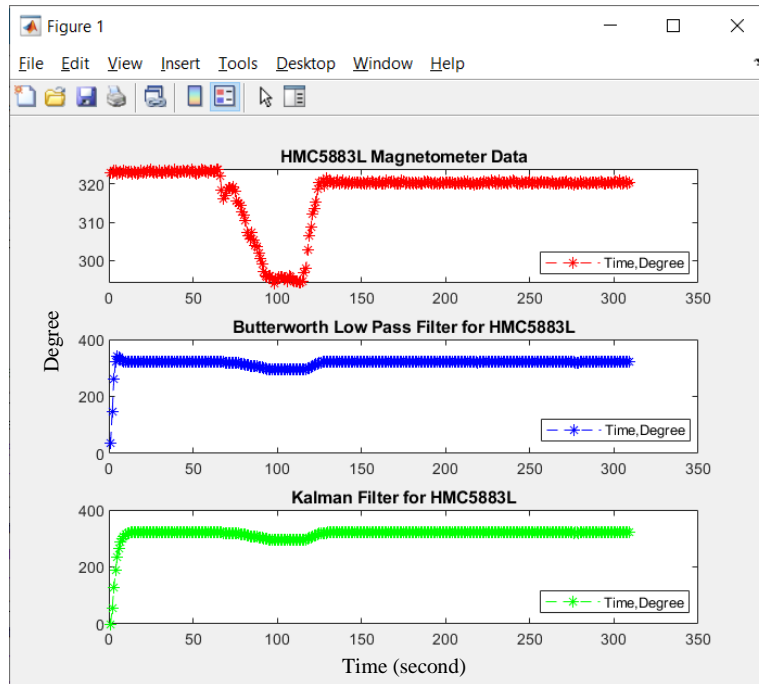

Figure 22. GPS data visualization

Figure 23. HMC5883L data visualization

Table 3. RMSE comparison

RMSE GPS (m)		RMSE HMC5883L (degree)	
Butterworth LPF	Kalman Filter	Butterworth LPF	Kalman Filter
0.0263888	0.1823068	0.8174105	1.0232198

Overall, the development process to create a two-wheeled hand tractor remote control system has been completed, but the automation process must be carried out. Therefore, a preliminary study was conducted using Simulink on kinematic model mapping and tractor movement simulation. As shown in (1) to (9) were then implemented into Simulink with two controller types. Figure 24 is a block diagram of the Pure Pursuit Control, while Figure 25 is a supervisory logic control with details in Figure 26. The parameters and values used in this simulation can be seen in Table 4. The waypoint concept is the basis of this simulation, where the input location is (x, y) in the form of a 10×2 array and forms a back-and-forth path. Details of each Simulink block can be seen in Figures 27 to 30.

Figure 31 illustrates the simulation of tractor movement using supervisory logic control, while Figure 32 simulates tractor movement using pure pursuit control. Meanwhile, Figures 33 and 34 depict each controller's right and left wheel speeds. From the simulation results, it can be concluded that supervisory logic control has a higher level of accuracy, reaching 10 out of 10 coordinates (100%), while pure pursuit control has 6 out of 10 coordinates (60%).
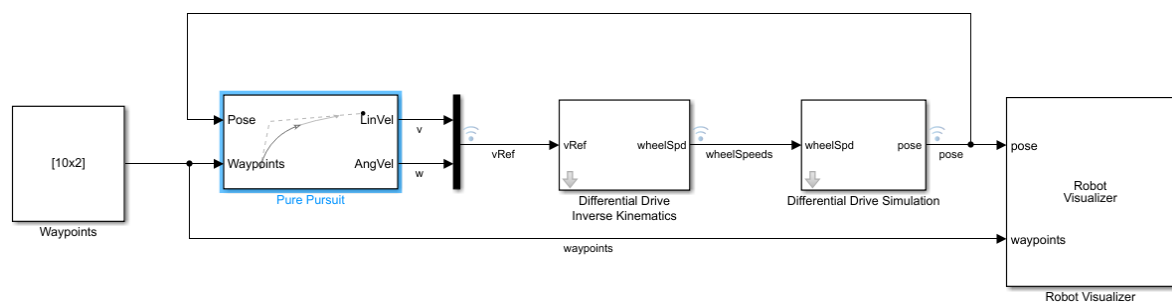

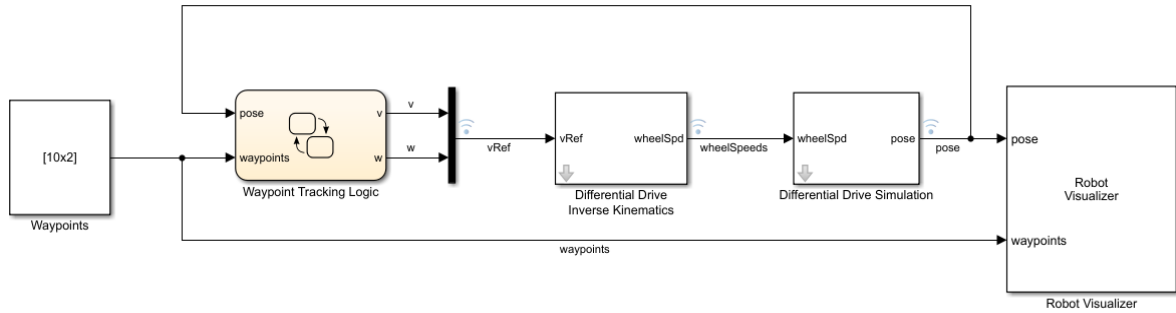Figure 24. Pure pursuit control Simulink block diagram

Figure 25. Supervisory logic control Simulink block diagram

Table 4. Simulation parameters

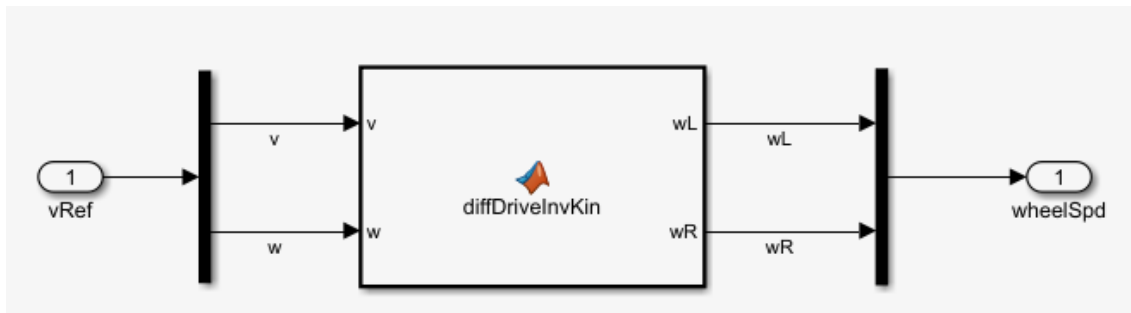| Parameters	Value
Desired linear velocity (v)	0.5 m/s
Maximum angular velocity (ω)	0.785 rad/s
Lookahead distance	0.35 m
L	1.6 m
R	0.4 m
Waypoints [x_1, y_1; …; x_n, y_n]	[0,0; 0,5; 1,5; 1,1; 2,1; 2,5; 3,5; 3,1; 4,1; 4,5]
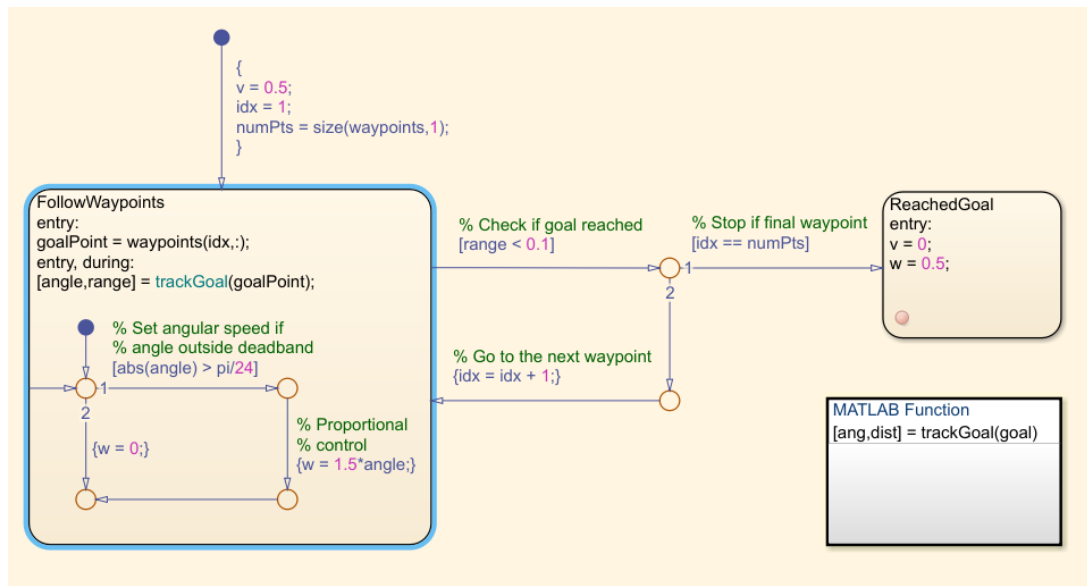
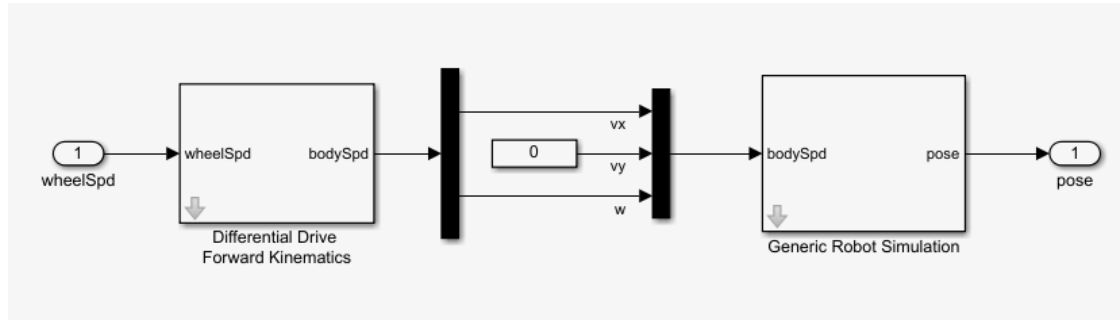Figure 26. Waypoint tracking supervisory logic

Figure 27. Differential drive inverse kinematics block detail

Figure 28. Differential drive simulation block detail
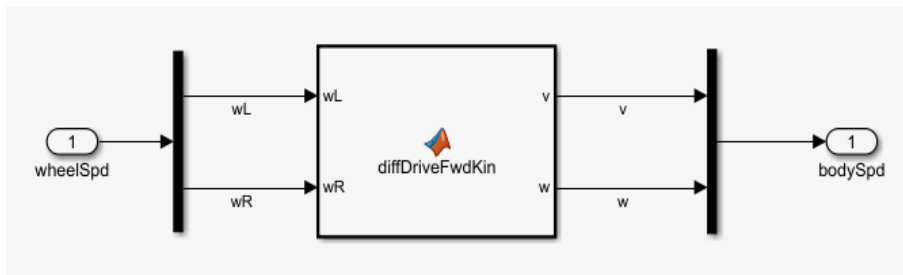

Figure 29. Differential drive forward kinematics block detail
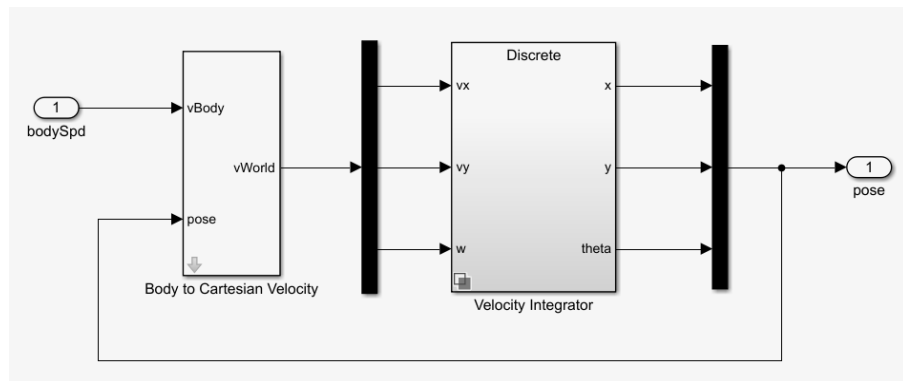

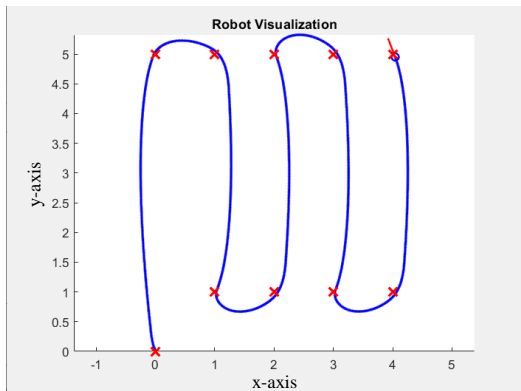Figure 30. Generic robot simulation block detail

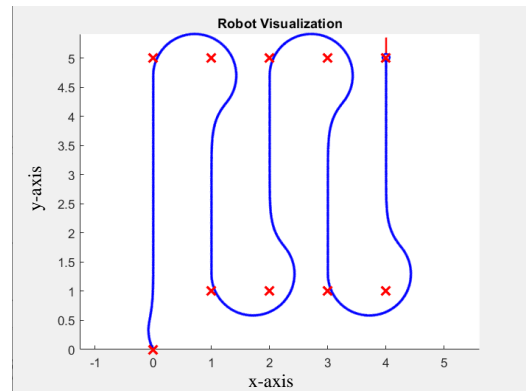Figure 31. Tractor movement simulation based on supervisory logic control

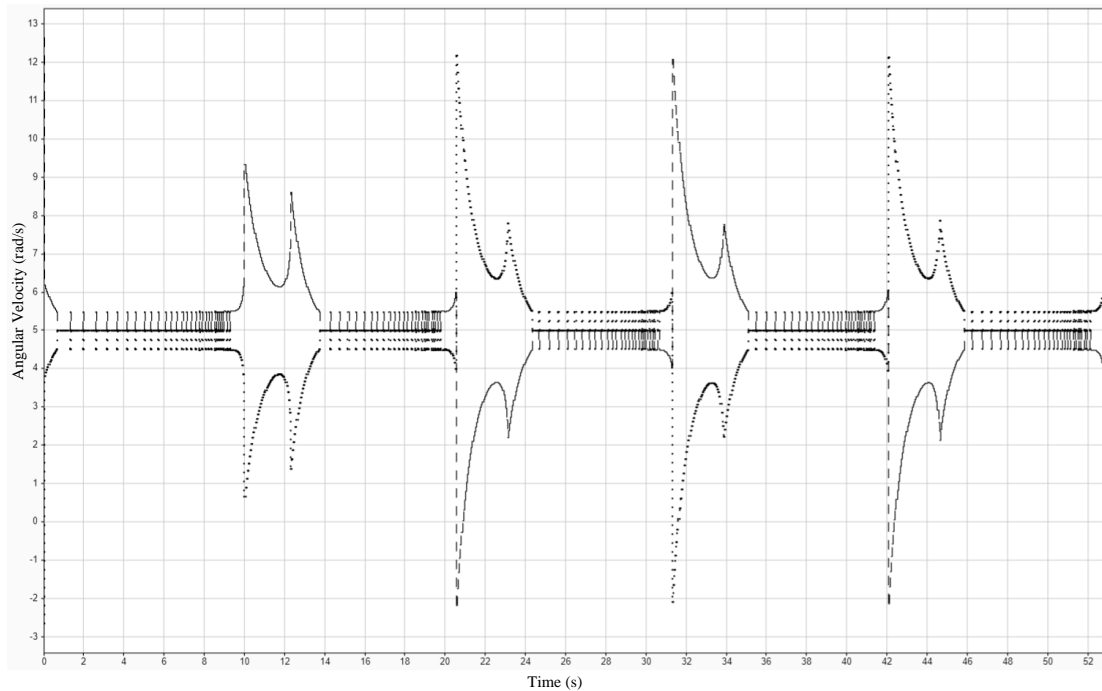Figure 32. Tractor movement simulation based on pure pursuit control

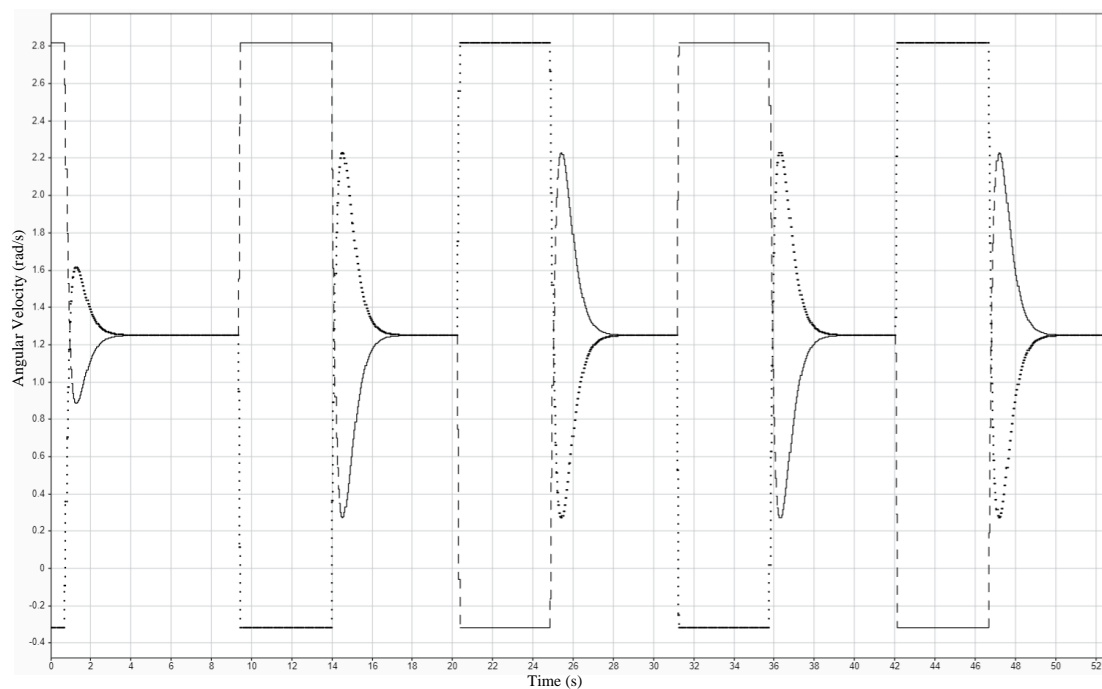Figure 33. Left and right wheel speed (supervisory logic control)

Figure 34. Left and right wheel speed (pure pursuit control)

4.   CONCLUSION

In conclusion, this study has presented a two-wheeled walk-behind tractor controlling system. The design and development process included mechanical modifications to the tractor, testing the functionality of the electronic component circuit, and integrating the electronic component circuit with the created software. The handlebar head was modified mechanically and electronically by adding several actuators to pull the clutch handle and move the steering linkage. A DC motor is then installed as a controlling actuator on the tension handle and throttle lever. The final modification to the main bar was the addition of a weight balancer

hanger to ensure that the tractor's front and rear loads were balanced. This system used Bluetooth to communicate between the actuator and the mobile application. The integration of software and electronic circuits has been completed successfully, allowing tractor operators to operate remotely. Numerous trials have been conducted to evaluate the tractor's movement in an open field. The field test was done in two phases: prototype and final product, to generate the low-cost controlling system of the two-wheeled tractor using low energy use. The test results show a cost efficiency of 21.74% and 84.62% battery usage efficiency for the final product. The prototype design has been put through its paces on a G 3000 tractor. Numerous analysis results and enhancements are obtained from this test, which is required to create more efficient cost and battery life products. Based on the first test results, mechanical and electronic design modifications have been made and tested on a tractor of the G1000 type, with improved outcomes. With this system, farmers no longer experience fatigue by controlling the hand tractor remotely.

In addition, preliminary studies were carried out to create mathematical models and simulations of tractor movements. This model is based on kinematics for differentially driven two-wheeled vehicles. The model moves in the direction specified by the coordinates (back and forth path). The simulation results show that supervisory logic control reaches 100%, better than pure pursuit control, which only gets 60% from the specified point. These two-controller algorithms are the results of simulations in the MATLAB/Simulink application and became a limitation of this research. We also collect data from GPS and compass sensors during the field trials using IoT technology. The raw data results have noise and are very unstable; therefore, Kalman and second-order Butterworth low pass filters are used. The RMSE test results show that the Butterworth LPF performance is better than the Kalman filter. Further research is needed to determine the effects of field tests on tractors.

REFERENCES

[1]   A. Syuhada, M. E. Armanto, A. Siswanto, M. Yazid, and E. Wildayana, "Food security and environmental sustainability on the south sumatra Wetlands, Indonesia," *Systematic Reviews in Pharmacy*, vol. 11, no. 3, pp. 457–464, 2020, doi: 10.5530/srp.2020.3.58.

[2]   M. Kragh *et al.*, "FieldSAFE: Dataset for obstacle detection in agriculture," *Sensors*, vol. 17, no. 11, Art. no. 2579, Nov. 2017, doi: 10.3390/s17112579.

[3]   J. Guo *et al.*, "Multi-GNSS precise point positioning for precision agriculture," *Precision Agriculture*, vol. 19, no. 5, pp. 895–911, Oct. 2018, doi: 10.1007/s11119-018-9563-8.

[4]   H. Wang and N. Noguchi, "Navigation of a robot tractor using the centimeter level augmentation information via Quasi-Zenith Satellite System," *Engineering in Agriculture, Environment and Food*, vol. 12, no. 4, pp. 414–419, Oct. 2019, doi: 10.1016/j.eaef.2019.06.003.

[5]   N. T. Binh, N. A. Tung, D. P. Nam, and N. H. Quang, "An adaptive backstepping trajectory tracking control of a tractor trailer wheeled mobile robot," *International Journal of Control, Automation and Systems*, vol. 17, no. 2, pp. 465–473, Feb. 2019, doi: 10.1007/s12555-017-0711-0.

[6]   K. Alipour, A. B. Robat, and B. Tarvirdizadeh, "Dynamics modeling and sliding mode control of tractor-trailer wheeled mobile robots subject to wheels slip," *Mechanism and Machine Theory*, vol. 138, pp. 16–37, 2019, doi: 10.1016/j.mechmachtheory.2019.03.038.

[7]   A. Fabbri, C. Cevoli, and G. Cantalupo, "A method for handlebars ballast calculation in order to reduce vibrations transmissibility in walk behind tractors," *Journal of Agricultural Engineering*, vol. 48, no. 2, pp. 81–87, Jun. 2017, doi: 10.4081/jae.2017.599.

[8]   B. Shyrokau *et al.*, "The effect of steering-system linearity, simulator motion, and truck driving experience on steering of an articulated tractor-semitrailer combination," *Applied Ergonomics*, vol. 71, pp. 17–28, Sep. 2018, doi: 10.1016/j.apergo.2018.03.018.

[9]   F. Susu *et al.*, "Design and prototype performance experiments of steering-by-wire hydraulic pressure system of tractor," *Nongye Gongcheng Xuebao/Transactions of the Chinese Society of Agricultural Engineering*, vol. 33, no. 10, pp. 86–93, 2017, doi: 10.11975/j.issn.1002-6819.2017.10.011.

[10]   P. Kassaeiyan, K. Alipour, and B. Tarvirdizadeh, "A full-state trajectory tracking controller for tractor-trailer wheeled mobile robots," *Mechanism and Machine Theory*, vol. 150, Aug. 2020, doi: 10.1016/j.mechmachtheory.2020.103872.

[11]   S. M. Shafaei, M. Loghavi, and S. Kamgar, "Fundamental realization of longitudinal slip efficiency of tractor wheels in a tillage practice," *Soil and Tillage Research*, vol. 205, p. 104765, Jan. 2021, doi: 10.1016/j.still.2020.104765.

[12]   A. Janulevičius, V. Damanauskas, and G. Pupinis, "Effect of variations in front wheels driving lead on performance of a farm tractor with mechanical front-wheel-drive," *Journal of Terramechanics*, vol. 77, pp. 23–30, Jun. 2018, doi: 10.1016/j.jterra.2018.02.002.

[13]   S. M. Shafaei, M. Loghavi, and S. Kamgar, "Ascertainment of driving lead of tractor front wheels as loaded by draft force," *Measurement*, vol. 165, Dec. 2020, doi: 10.1016/j.measurement.2020.108134.

[14]   S. M. Shafaei, M. Loghavi, and S. Kamgar, "Development and implementation of a human machine interface-assisted digital instrumentation system for high precision measurement of tractor performance parameters," *Engineering in Agriculture, Environment and Food*, vol. 12, no. 1, pp. 11–23, Jan. 2019, doi: 10.1016/j.eaef.2018.08.006.

[15]   H. Wang and N. Noguchi, "Adaptive turning control for an agricultural robot tractor," *International Journal of Agricultural and Biological Engineering*, vol. 11, no. 6, pp. 113–119, 2018, doi: 10.25165/j.ijabe.20181106.3605.

[16]   M. Xiao, J. Zhao, Y. Wang, H. Zhang, Z. Lu, and W. Wei, "Fuel economy of multiple conditions self-adaptive tractors with hydro-mechanical CVT," *International Journal of Agricultural and Biological Engineering*, vol. 11, no. 3, pp. 102–109, 2018, doi: 10.25165/j.ijabe.20181103.2158.

[17]   J. Han, C. Xia, G. Shang, and X. Gao, "In-field experiment of electro-hydraulic tillage depth draft-position mixed control on tractor," *IOP Conference Series: Materials Science and Engineering*, vol. 274, Dec. 2017, doi: 10.1088/1757-899X/274/1/012028.

[18]   C. Gupta, V. K. Tewari, A. Ashok Kumar, and P. Shrivastava, "Automatic tractor slip-draft embedded control system," *Computers and Electronics in Agriculture*, vol. 165, Oct. 2019, doi: 10.1016/j.compag.2019.104947.

[19]   J. Tarighi and S. S. Mohtasebi, "Design, fabrication and evaluation a new mechanism to automatic weight transfer control system on a tractor," *Emirates Journal for Engineering Research*, vol. 26, no. 2, 2021.

[20]   X. Yin, Y. Wang, Y. Chen, C. Jin, and J. Du, "Development of autonomous navigation controller for agricultural vehicles," *International Journal of Agricultural and Biological Engineering*, vol. 13, no. 4, pp. 70–76, 2020, doi: 10.25165/j.ijabe.20201304.5470.

[21]   H. Zhou *et al.*, "Design and test of laser-controlled paddy field levelling-beater," *International Journal of Agricultural and Biological Engineering*, vol. 13, no. 1, pp. 57–65, 2020, doi: 10.25165/j.ijabe.20201301.4989.

[22]   Y. Ding *et al.*, "Novel low-cost control system for large high-speed corn precision planters," *International Journal of Agricultural and Biological Engineering*, vol. 14, no. 2, pp. 151–158, 2021, doi: 10.25165/j.ijabe.20211402.6053.

[23]   A. Das, M. Ghosal, and D. Das, "Studies on applications of electronics in wheel slip control of agricultural tractor," *International Journal of Chemical Studies*, vol. 8, no. 2, pp. 1483–1487, Mar. 2020, doi: 10.22271/chemi.2020.v8.i2w.8970.

[24]   S. Soylu and K. Çarman, "Fuzzy logic based automatic slip control system for agricultural tractors," *Journal of Terramechanics*, vol. 95, pp. 25–32, Jun. 2021, doi: 10.1016/j.jterra.2021.03.001.

[25]   S. M. Shafaei, M. Loghavi, and S. Kamgar, "Benchmark of an intelligent fuzzy calculator for admissible estimation of drawbar pull supplied by mechanical front wheel drive tractor," *Artificial Intelligence in Agriculture*, vol. 4, pp. 209–218, 2020, doi: 10.1016/j.aiia.2020.10.001.

[26]   S. M. Shafaei, M. Loghavi, and S. Kamgar, "An extensive validation of computer simulation frameworks for neural prognostication of tractor tractive efficiency," *Computers and Electronics in Agriculture*, vol. 155, pp. 283–297, Dec. 2018, doi: 10.1016/j.compag.2018.10.027.

[27]   C. Wu, Z. Chen, D. Wang, Z. Kou, Y. Cai, and W. Yang, "Behavior modelling and sensing for machinery operations using smartphone's sensor data: A case study of forage maize sowing," *International Journal of Agricultural and Biological Engineering*, vol. 12, no. 6, pp. 66–74, 2019, doi: 10.25165/j.ijabe.20191206.4702.

[28]   R. Ospina and N. Noguchi, "Improved inclination correction method applied to the guidance system of agricultural vehicles," *International Journal of Agricultural and Biological Engineering*, vol. 13, no. 6, pp. 183–194, 2020, doi: 10.25165/j.ijabe.20201306.6012.

[29]   D. Kapsalis, O. Sename, V. Milanes, and J. J. Martinez Molina, "Design and experimental validation of an LPV pure pursuit automatic steering controller," *IFAC-PapersOnLine*, vol. 54, no. 2, pp. 63–68, 2021, doi: 10.1016/j.ifacol.2021.06.010.

[30]   G. C. Rains, A. G. Faircloth, C. Thai, and R. L. Raper, "Evaluation of a simple pure pursuit path-Following algorithm for an autonomous, articulated-steer vehicle," *Applied Engineering in Agriculture*, vol. 30, no. 3, pp. 367–374, Jul. 2014, doi: 10.13031/aea.30.10347.

[31]   N. Mebarki, T. Rekioua, Z. Mokrani, and D. Rekioua, "Supervisor control for stand-alone photovoltaic/hydrogen/ battery bank system to supply energy to an electric vehicle," *International Journal of Hydrogen Energy*, vol. 40, no. 39, pp. 13777–13788, Oct. 2015, doi: 10.1016/j.ijhydene.2015.03.024.

[32]   M. Tomera, "Hybrid real-time way-point controller for ships," in *2016 21st International Conference on Methods and Models in Automation and Robotics (MMAR)*, Aug. 2016, pp. 630–635, doi: 10.1109/MMAR.2016.7575209.

[33]   K. N. Dewangan and V. K. Tewari, "Characteristics of hand-transmitted vibration of a hand tractor used in three operational modes," *International Journal of Industrial Ergonomics*, vol. 39, no. 1, pp. 239–245, Jan. 2009, doi: 10.1016/j.ergon.2008.08.007.

[34]   F. Shiotsu *et al.*, "Initiation and dissemination of organic rice cultivation in Bali, Indonesia," *Sustainability*, vol. 7, no. 5, pp. 5171–5181, Apr. 2015, doi: 10.3390/su7055171.

[35]   B. Lakitan *et al.*, "Inclusive and ecologically-sound food crop cultivation at tropical non-tidal wetlands in Indonesia," *AGRIVITA Journal of Agricultural Science*, vol. 41, no. 1, Feb. 2019, doi: 10.17503/agrivita.v40i0.1717.

[36]   U. Paman, S. Uchida, and S. Inaba, "Economic potential of tractor hire business in Riau Province, Indonesia: A case study of small tractors for small rice farms," *Agricultural Engineering International: CIGR Journal*, vol. 12, no. 1, pp. V-Management, Ergonomics and Systems Engineering, 2010.

[37]   Q. Li, R. Li, K. Ji, and W. Dai, "Kalman Filter and its application," in *2015 8th International Conference on Intelligent Networks and Intelligent Systems (ICINIS)*, Nov. 2015, pp. 74–77, doi: 10.1109/ICINIS.2015.35.

[38]   V. K. Ingle and J. G. Proakis, *Digital signal processing using MATLAB ® Third Edition*. Third. Stamford: Cengage Learning, 2012.

[39]   R. Siegwart, I. R. Nourbakhsh, and D. Scaramuzza, *Introduction to autonomous mobile robots*. The MIT Press, 2011.

[40]   J. Liu and G. Guo, "Vehicle localization during GPS outages with extended Kalman Filter and deep learning," *IEEE Transactions on Instrumentation and Measurement*, vol. 70, pp. 1–10, 2021, doi: 10.1109/TIM.2021.3097401.

BIOGRAPHIES OF AUTHORS

Padma Nyoman Crisnapati ⓘD 🔢 SC ◯ earned his bachelor's degree in 2009 from the Department of Informatics Engineering at Sepuluh Nopember Institute of Technology. He then pursued a master's degree in 2011 from Ganesha Education University in the Learning Technology program and a master's degree in Computer Science in 2018 from Ganesha Education University. Working as a permanent lecturer at the STIKOM Bali Institute of Technology and Business, teaching sensors transducer, assembly language, and animation, and has served as Head of the Computer Systems Study Program from 2016 to 2020. He is now pursuing a doctorate in the Mechatronics Engineering department at Rajamangala University of Technology Thanyaburi (RMUTT). His research interests include 2D and 3D animation, the internet of things, robotics, automation, augmented and virtual reality, and robotics. He can be reached via email: padma_c@mail.rmutt.ac.th or crisnapati@stikom-bali.ac.id.

Dechrit Maneetham ⓘ 🄶 🆂 ⓒ is an Associate Professor of Mechatronics Engineering at the Rajamangala University of Technology in Thanyaburi, Thailand. He earned his B.Tech. and M.S. degrees in electrical and computer engineering from the King Mongkut's University of Technology in North Bangkok, a D.Eng. in Mechatronics from the Asian Institute of Technology in 2010, and a PhD in Electrical and Computer Engineering from Mahasarakham University in 2018. Dr Dechrit is the author or co-author of over 30 technical papers and has taught short robotics courses at various conferences. Additionally, he has authored seven books, including Pneumatics System, Hydraulics System, MCS-51 Microcontroller, PIC Microcontroller, Arduino Microcontroller, PLC Beckhoff, and Robot. He has over 15 years of experience teaching engineering and researching robotics, automation, mechatronics, and biomedical applications. His research interests include biomedical applications, robotics and automation, and mechatronics applications. He can be contacted at email: dechrit_m@rmutt.ac.th.

Evi Triandini ⓘ 🄶 🆂 ⓒ holds a bachelor's degree in Agricultural Cultivation from Brawijaya University in Malang. The Asian Institute of Technology in Bangkok, Thailand, offers a Master of Science in Information Management. Surabaya's Sepuluh Nopember Institute of Technology (ITS) offers a doctoral program in computer science. Among the research, fields are software engineering, information systems, and e-commerce. She is currently a member of the Indonesian Computer, Electronics, and Instrumentation Support Society (IndoCEISS) and Cooperation Research Inter University's central board (CORIS). IEEE and The International Association of Engineers member (IAENG). Her research interest includes software engineering, e-commerce, and information systems. She can be contacted at email: evi@stikom-bali.ac.id.